

An Attempt to Observe Debris from the Breakup of a Titan 3C-4 Transtage

E. S. Barker, M. J. Matney

*National Aeronautics and Space Administration, Johnson Space Center, Mail Code KX,
Houston, TX 77058, USA, 281-483-2591, FAX 281-483-5276, edwin.s.barker@nasa.gov*

T. Yanagisawa

*Japan Aerospace Exploration Agency
7-44-1 Jindaiji-higashi-machi, Chofu, Tokyo, 182-8522 Japan*

J.-C. Liou, K. J. Abercromby, H. M. Rodriguez, M. F. Horstman

ESCG, 2224 Bay Area Blvd, Houston, TX, 77058, USA

P. Seitzer

University of Michigan, Dept. of Astronomy, 818 Dennison Bldg. Ann Arbor, MI 48109-1090, USA

ABSTRACT

In February 2007 dedicated observations were made of the orbital space predicted to contain debris from the breakup of the Titan 3C-4 transtage back on February 21, 1992. These observations were carried out on the Michigan Orbital DEbris Survey Telescope (MODEST) in Chile with its 1.3° field of view. The search region or orbital space (inclination and right ascension of the ascending node) was predicted using NASA's LEGEND (LEO-to-GEO Environment Debris) code to generate a Titan debris cloud. Breakup fragments are created based on the NASA Standard Breakup Model (including fragment size, area-to-mass, and delta-V distributions). Once fragments are created, they are propagated forward in time with a subroutine, GEOPROP. Perturbations included in GEOPROP are those due to solar/lunar gravity, radiation pressure, and major geopotential terms. Barker, et al. al, 2006 [1] used similar LEGEND predictions to correlate survey observations made by MODEST in February 2002 and found several possible night-to-night correlations in the limited survey dataset.

One conclusion of the survey search [1] was to dedicate a MODEST run to observing a geosynchronous region predicted to contain debris fragments and actual Titan debris objects (SSN 25000, 25001 and 30000). Such a dedicated run was undertaken with MODEST between February 17 and 23, 2007 (UT dates). MODEST's limiting magnitude of 18.0 (S/N~10) corresponds to a size of 28 cm assuming a diffuse Lambertian albedo of 0.13. However, based on observed break-up data, we expect most debris fragments to be smaller than 22 cm, which implies a need to increase the effective sensitivity of MODEST for smaller objects. MODEST's limiting size could not be lowered by increasing the exposure time from 5 to 20 seconds due to trailing of the image. However, special image processing did allow the detection of smaller debris. Special processing combined several individual CCD images to detect faint objects that were invisible on a single CCD image. Sub-images are cropped from six consecutive CCD images with pixel shifts between images being consistent with the predicted movement of a Titan object. A median image of all the sub-images is then created leaving only those objects with the proper Titan motion. Limiting the median image in this manner brings the needed computer time to process all images taken on one night down to about 50 hours of CPU time.

Successful observations were carried out over six consecutive nights. Positions for each of the 62 detected targets on individual nights were fit under the assumption of circular orbits. Those targets that were observed on other nights and that had similar ACO orbital parameters will be combined and their observed positions fit to a full six parameter orbit. Combinations of targets having RMS fits less than ~10 arcseconds were considered to be the same target. Six combinations were correlated to cataloged targets (CTs). Cataloged Titan debris (SSNs 25000, 25001, 30000) was not detected because they were not observable during night hours. Nine combinations could not be correlated to cataloged targets; hence they were defined as uncataloged targets (UCTs). These UCTs have orbital elements very similar to those predicted by LEGEND and thus are strong candidates for Titan debris.

1. INTRODUCTION

1.1 Titan Breakup Event

The breakup of the Titan 3C-4 transtage occurred on February 21, 1992 at an altitude of ~35,600 km, inclination (INC) of 11.9 degrees and a right ascension (RA) of 21.8 hours. The operator of the GEODSS sensor on Maui, Hawaii witnessed approximately 20 pieces in the breakup, but none were tracked at the time. Subsequent to the breakup the U. S. Space Surveillance Network (SSN) identified three pieces of the debris and assigned them to the catalogue as SSN25000, SSN25001 and SSN30000.

1.2 MODEST Survey

Since 2001, the National Aeronautics and Space Administration (NASA) has carried out an optical survey of the debris environment in the geosynchronous earth orbit (GEO) region with the Michigan Orbital Debris Survey Telescope (MODEST) in Chile. MODEST is a 0.6/0.9-m Schmidt telescope located at the Cerro Tololo Inter-American Observatory (CTIO) in Chile. A brief description of the system follows: for more details see [2, 3]. The telescope is equipped with a thinned 2048 x 2048 pixel charge couple device (CCD) with a field of view (fov) of 1.3° square and 2.318 arc-second pixels. In a 5 second exposure through a broad R filter, a limiting magnitude 18 in R is reached with a signal to noise (S/N) of 10.

The primary purpose of the MODEST system has been to operate in survey mode to sample uniformly the GEO belt and regions above and below it on at least a semi-annual basis. In survey mode, the telescope tracks at the sidereal rate a fixed right ascension (RA) and declination (DEC) point close to the anti-solar point just outside of Earth shadow. The primary DEC chosen for each run is the declination of the GEO belt as seen from Cerro Tololo for that date. On additional nights the telescope is pointed at DEC positions above and below the GEO belt. The declinations are chosen with overlapping field of views (FOV) and usually are concentrated on regions known to have significant cataloged target (CT) populations, hence potential debris sources. During the exposure the charge on the CCD is shifted backwards such that GEO objects appear as point sources or short streaks, and stars appear as fixed length streaks. During the 5.3 minutes it takes a station-keeping GEO object to drift across the FOV, eight independent detections can be made. A minimum of four detections are required in this 5.3 minute window for a real object. All correlated objects are visually examined to guard against false detections.

1.3 Calculation of Orbital Parameters Assuming a Circular Orbit

Fitting a set of angles-only observations has been a long-standing problem in astrodynamics since the early days of astronomy. Historically, orbits are defined by six-dimensional Kepler elements (there are several ways to represent these elements – all equivalent – but a typical set consists of the semi-major axis, eccentricity, inclination, ascending node, argument of perigee, and true anomaly, all at a given epoch). However, “moving around” in this six-dimensional space to optimize a data fit presents a number of difficulties. Kepler elements have singularities in their derivatives, and even specialized “non-singular” elements have potential problems. There is a way of representing a state vector of an orbit that is non-singular, however, and that is by using Cartesian coordinates. There is a one-to-one correspondence between a six-dimensional Cartesian state vector (3 dimensions of position, 3 of velocity) and a set of Kepler elements, so any set of Cartesian state vectors can be easily converted into conventional Kepler elements, and *vice versa*.

Our orbit fit program uses an all-purpose multidimensional optimization routine known as a simplex method taken from Numerical Recipes [4]. While not always the most efficient method, it is robust enough to use with any data configuration. For a set of short-arc observations, an epoch time is chosen (such as the epoch of the first observation). Different six-dimensional Cartesian vectors are tested by transforming each into Kepler orbits, propagating them to each observation time in the set of observations, and computing the differences between the predicted and observed look angle vectors. One obvious way to measure this difference is to take the arc cosine of the vector dot product of the two normalized look vectors. However, if the angle between the vectors is small, the dot-product is very close to 1.0, and can lead to round off problems. Instead, we use the vector difference between the two normal vectors. This gives an excellent approximation of the angle between the two vectors if they are sufficiently close and can be transformed into a positional error on the sky in arc seconds. The optimization routine “experiments” with various Cartesian coordinate configurations until the sum of the squares of the positional errors (DVEC) is minimized. DVEC is used as a measure of the accuracy of the fit in arcseconds.

Because the observation arcs are so short, there are in general a variety of different orbits (of varying eccentricity) that give relatively good fits to the data, making it difficult to determine a single optimal orbit with no constraints on the solution. Therefore, the current configuration of the software penalizes solutions by how far their eccentricities differ from zero. This penalty is added to the positional error described above, resulting in an optimized solution equivalent to the best-fit circular orbit to the data set. We define this best-fit circular orbit as the assumed circular orbit (ACO) solution because the software has severely penalized any solution where eccentricity is greater than 0. Similarly, we define the eccentric orbit solution as one where the software penalties have been removed and the eccentricity has been allowed to vary.

2. MODEST DATASET

2.1 MODEST Observational Data Set

Using the actual Two Line Element (TLE) sets for the CTs and the ACO orbital elements for the uncataloged targets (UCTs), we plot the population distributions for all MODEST data collected in normal survey mode from 2004 – 2007 in different formats shown in Figs. 1 and 2. The GEO belt region is shown as the concentration of blue points on the horizontal axis with INC values less than 0.1° . The major feature seen in Fig. 1, starting at 15° inclination (INC) and 0° right ascension of the ascending node (RAAN) and following decreasing INC and up to 90° in RAAN is caused by the precession of the orbital planes due to the Earth's oblateness plus the solar and lunar perturbations on the orbital planes. As uncontrolled CTs and debris are gravitationally perturbed their inclinations increase and they move away from the GEO belt to a maximum INC of about 15° over ~ 50 years. This evolution is along predictable patterns, particularly evident in their INC and RAAN distributions. Another way to display the INC and RAAN distributions is with a polar or the angular momentum plot as shown in Fig. 2 which is limited to just the UCTs or primarily debris targets.

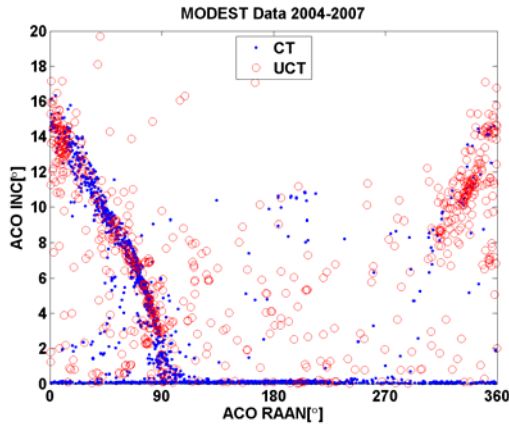


Fig. 1. MODEST CTs and UCTs for 2004-2007.

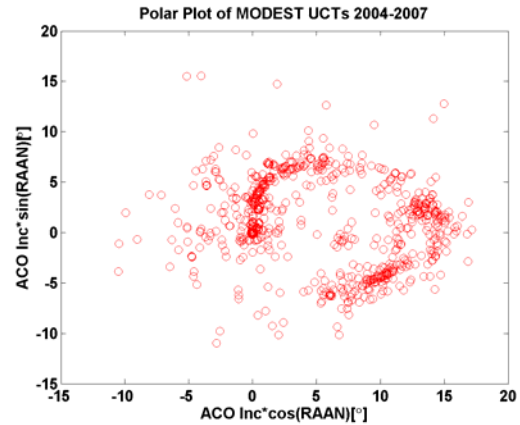


Fig. 2. Polar plot of data presented in Fig. 1 but limited to just UCTs.

There are several clusters (Schildknecht [5] has used a “cloud” nomenclature) of INC and RAAN in observed distributions as shown in Figs. 1 and 2. Identification of the source(s) for these clusters of UCTs would be advantageous to the overall definition of the GEO orbital debris environment. The remainder of this paper will present arguments for the identity of the source of the clustering of UCTs roughly centered on an $INC=11^\circ$ and a $RAAN=335^\circ$ as seen in Fig. 1 or in Fig. 2 near x and y values of 9.5° and -5.0° , respectively. In Fig. 3 the INC and RAAN plot has the horizontal axis redefined to better illustrate the clustering around 0° or 360° . The limited data MODEST UCT dataset is shown in Fig. 4 where the Titan sample box is somewhat larger than the actual clustering of UCTs to make sure we are sampling all the possible UCT and LEGEND debris correlations. The parent body of the Titan breakup (SSN 3432) has values of $INC=10.4^\circ$ and $RAAN=333.53^\circ$ for a 2007 epoch.

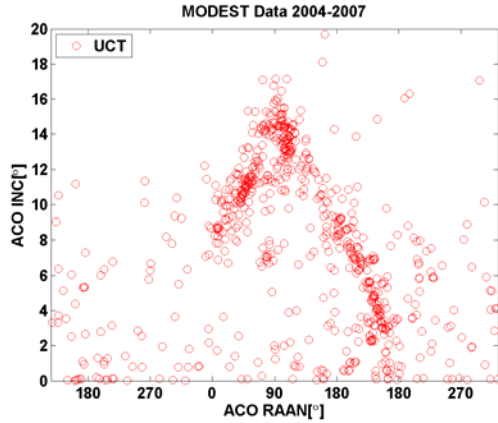


Fig. 3. Inc vs. RAAN plot for MODEST 2004-2007 UCTs, same plot as Fig. 1 except for shifted horizontal axis.

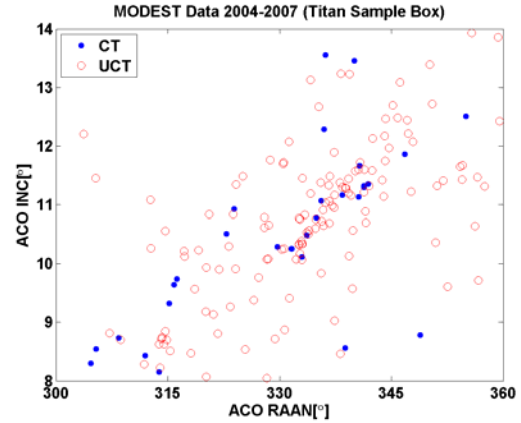


Fig. 4. Inc vs. RAAN plot for MODEST 2004-2007, same plot as Fig. 1 but limited to the Titan sample box around RAAN=330°, INC=11°

3. LEGEND MODELING

3.1 Description of LEGEND

NASA's orbital debris evolutionary model LEGEND (LEO-to-GEO Environment Debris) is capable of simulating the historical and future debris populations in the near-Earth environment [6, 7]. The historical part of LEGEND adopts a deterministic approach to mimic historical launches and known breakup events. Instead of modeling the whole environment, LEGEND can also be simplified to simulate an individual event, and has been chosen as the tool for providing predicted Titan fragments for this study. Once the breakup event is specified in LEGEND, fragments down to 1 mm in size are created with the NASA Standard Breakup Model, which describes the fragment size, area-to-mass ratio (A/M), and velocity distributions [8]. All objects are propagated forward in time after breakup. Perturbations included in the GEO propagator, GEOPROP, include solar and lunar gravitational perturbations, solar radiation pressure, and Earth gravity-field zonal (J_2 , J_3 , J_4) and tesseral ($J_{2,2}$, $J_{3,1}$, $J_{3,3}$, $J_{4,2}$, $J_{4,4}$) perturbations. The simulated orbital elements and other physical properties of the fragments are stored in output files for additional post-processing analysis. The modeled Titan fragments described in this paper were generated from a special LEGEND simulation. Figs. 5 and 6 demonstrate the loci of debris created with sizes greater than 10cm for February 2007. Two-hundred thirty-eight Titan fragments 10 cm and larger were produced, and then propagated from the breakup date to day 51 of 2007 for comparison with the MODEST UCT data. In Figs. 5 and 6 these LEGEND propagated Titan fragments are plotted in black over the UCTs observed by the MODEST survey during the 2004-2007 period.

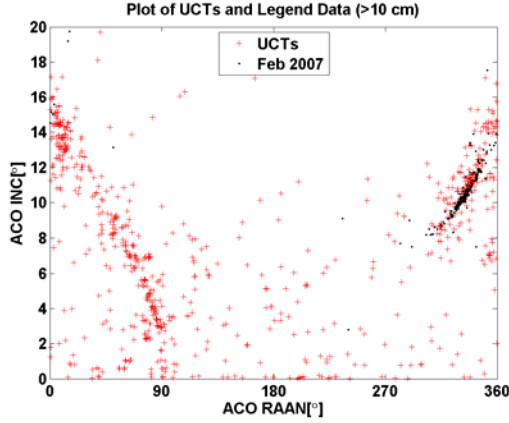


Fig. 5 Inclination- RAAN plot of potential debris predicted by the LEGEND modeling (>10cm) for February 2007. UCTs were observed during the MODEST survey (2004-2007).

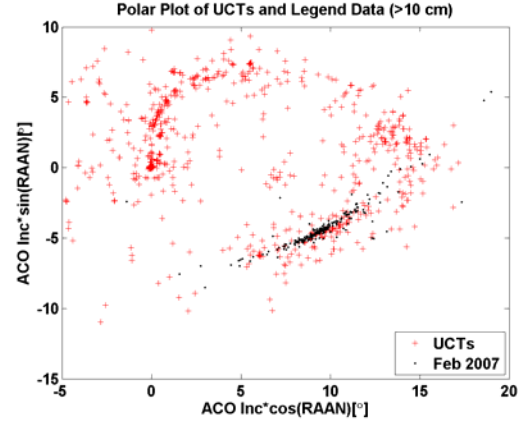


Fig. 6. Polar plot of potential debris predicted by the LEGEND modeling (>10cm) for February 2007. UCTs were observed during the MODEST survey (2004-2007)

4. DETECTION ALGORITHM

In order to detect Titan fragments, we used the new algorithm due to the faintness of objects. The algorithm uses several CCD frames to detect faint Titan objects that are invisible on a single CCD image. The observation sequence is a 20 second exposure every 53 seconds as the telescope tracks a position of constant right ascension and declination. The CCD camera attached to the telescope uses TDI mode during the exposure to match the motion of GEO objects. Therefore, GEO objects appear as point sources and field stars as horizontal streaks. The orbits of Titan fragments should have inclinations of about 10° ; therefore, they appear as inclined or nearly vertical streaks. Increasing the MODEST exposure time from 5 to 20 seconds did not improve the S/N because the Titan fragments were still trailed on an ever increasing sky background. As the time interval between each frame is 53 seconds, typical Titan fragments appear on six serial frames. Six frames are available to improve a signal-to-noise ratio for the detection of unresolved Titan fragments.

Active removal of the star streaks before stacking subframes is preferable because only six frames are available for the analysis. In order to do this, a median frame made of six sequential frames is subtracted from the each of the individual frames. By the characteristic of median algorithm, images of GEO debris are removed in the median frame and only streaks of stars remain. Subtracting this median image from each frame removes star streaks. Although some influences remains near the streaks of bright stars, these influences are effectively eliminated by patching the mask pattern image made of the median image. After applying the streak process to all the frames, the rest of the analysis was carried out using the stacking algorithm.

In order to detect Titan objects near or below the sky background, various shift values of Titan objects must be investigated. As we know the rough orbit of the Titan fragments from LEGEND models, the size of the shift value that must be investigated is relatively low as compared with the detection of regular GEO debris which has no a-priori orbital information. Shift values were bounded by the apparent RA-DEC rate box (RA: -1.09 to +0.87 arcsec/sec; DEC: -2.79 to -3.33 arcsec/sec) which was characteristic of the LEGEND predicted fragments. First, sub-frames are cropped from six sequential CCD frames to fit the predicted angular movement of a Titan object. A median image of all the sub-frames is then created. Using the average is slightly more powerful than the median in respect of the detection of unresolved objects. However, the median has the advantage of eliminating extremely high noise signatures, such as cosmic rays and hot pixels that remain in an average image. In this process, photons from the potential Titan object fall on the same pixels of sub-frames. This also improves the signal-to-noise ratio enabling one to detect unresolved Titan objects. In the median image, the stacking algorithm finds candidates of Titan objects using a threshold value and a parameter concerning to the candidate's shape. Limiting the formation of the median image to only those pixels shifts characteristic of Titan fragments brought the needed computer time to

process all images (~500) taken on one night down from weeks to about 50 hours of CPU time. Fig. 7 shows parts of six sequential frames around one of detected Titan fragments (A, section 6) and the median image for the first night. Although the object is dim and not well defined in the six sequential subframes, it is clearly recognized in the median image.

Using six frames and this algorithm, the detection limit is increased by 0.8-magnitude fainter than usual method. The detection threshold value should be determined carefully. If the analysis goal is for very faint Titan fragments, the threshold value must be low, which allows for the possible detection of many false candidates and be a time-consuming analysis. For this analysis, 3.5 times of the sky background noise was used for the threshold value. All of the processes are constructed with Perl scripts and IRAF (Image Reduction and Analysis Facility) software [9]. A more detailed description of the algorithm can be found in Yanagisawa, et al. [10].

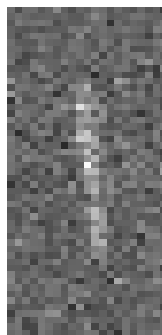
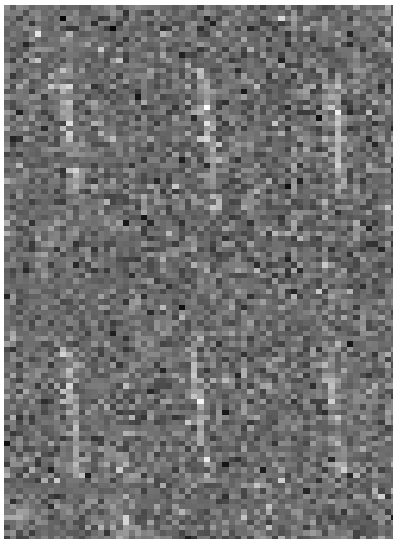


Fig. 7. Potential Titan fragment. The left figure shows parts of six individual, sequential subframes around candidate (A) and the right figure shows the median image of the six subframes. The total V magnitude for the trailed, median image is 17.84 ± 0.15 on DOY 049.

5. NEW OBSERVATIONS

Successful observations were carried out over six consecutive nights in February 2007. The observational procedure was to observe the same field (RA=10h 19m and DEC= $4^{\circ} 30'$) during the time the field was available. This field was chosen because the predicted orbits of the LEGEND generated, Titan fragments (see section 3.1) crossed the MODEST field of view during the observing period and the solar phase angle was as small as practical.

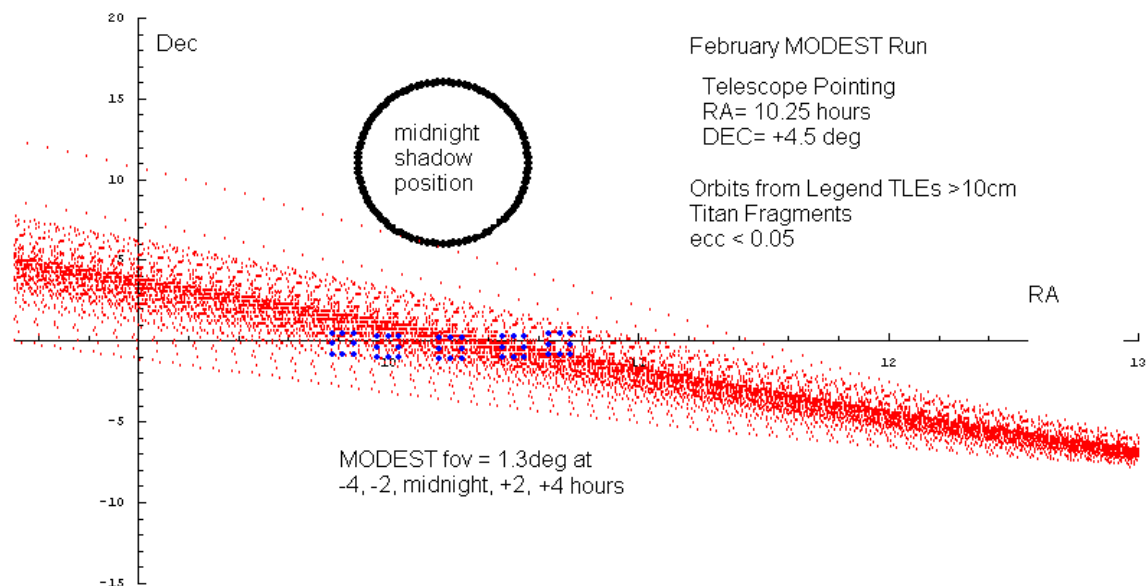


Fig. 8 Positions of the MODEST field of view and the LEGEND generated orbits for Titan fragments.

These orbits are demonstrated in Fig. 8 shown against a coordinate system fixed to the RA and DEC of the Earth's shadow at local midnight. The projected location of the MODEST field of view in this special coordinate system is shown as blue boxes for five times during the night. MODEST observations are routinely made as close to the Earth's shadow as possible because the solar phase angle is smaller, hence the solar illuminated debris is brighter.

Normal MODEST processing was carried out on the 20 sec frames and the detected moving targets were correlated against the Space Surveillance Network (SSN) catalog yielding the total number of targets shown in Table 1. Since the objective of the observational program was to detect the faintest targets, the dataset for the 6 nights was processed with the detection algorithm defined in Section 4. Since the stacking process yielded only one image from which to determine measured positions, two positions were determined from the first and last image that were stacked together. All of the images in the stack were referenced to the first image in the sequence whose coordinates and Johnson V magnitude were determined from the stars in the field by standard methods [11] with an uncertainty of about ± 0.15 magnitude. The position of the last image in the sequence was determined from the shifts in RA and DEC from the reference or first image of the sequence. These two positions for each of the 62 detected targets on individual nights were fit under the assumption of circular orbit (ACO) using the method described in section 1.3. Those targets that were observed on other nights and that had similar ACO orbital parameters (inclination, RAAN and mean motion) were combined and their observed positions fit to a full 6 parameter orbit or our eccentric orbit solution (section 1.3), which allowed the eccentricity to vary.

Combinations of targets having DELVEC fits less than ~ 10 arcseconds for a full 6 parameter orbit were considered to be the same target. Six combinations were correlated or linked to cataloged targets (CTs) in the U. S. Space Surveillance Catalog. Cataloged pieces of Titan debris (SSNs 25000, 25001, 30000) were not detected because they were not observable during night time hours. Nine combinations could not be linked to cataloged objects so they were defined as UCTs and are potential candidates for Titan debris. These combinations are summarized in Table 1.

Table 1. MODEST Observations Used in this Analysis

| DOY in 2007 | Observing Interval (hours) | Total Targets Detected in Field of View | Targets found by Detection Algorithm | Linked Correlated Targets | Linked Titan Fragments |
|----------------|----------------------------------|---|--|---------------------------------|------------------------------|
| 49 | 7.1 | | 10 | 5 | 3 |
| 50 | 7.7 | | 11 | 5 | 3 |
| 51 | 7.3 | | 15 | 5 | 6 |
| 52 | 2.9 | | 7 | 0 | 3 |
| 53 | 7.1 | | 12 | 4 | 4 |

| | | | | | |
|---------|-----|--|----|----------|----------|
| 54 | 7.3 | | 7 | 4 | 1 |
| summary | --- | | 62 | 6 unique | 9 unique |

6. DISCUSSION OF CORRELATIONS

The full six parameter orbit fits for the CTs are summarized in Table 2 along with the Two Line Element (TLE) sets for the epoch of the MODEST observations. Since the observations are for a short periods (< 5 minutes) separated by ~24 hours, the eccentricity values are not well determined. We have not presented the values for the argument of perigee or mean anomaly because the epoch of the TLEs does not correspond the epoch of the orbital fit. The single night fit for SSN 2867 is an ACO orbital fit. The differences in the orbital parameters for the other fits are indicative of the errors involved by fitting an orbit with sparse observations spaced approximately 1 day apart and basically the same portion of the orbit. An albedo of 0.13[12] and a diffuse Lambertian disk were assumed to convert the Johnson V magnitude into a characteristic length (Lc). No comparison with radar determined dimensions has been made because of the scarcity and uncertainties in the radar cross sections for GEO objects.

Table 2. Linked Correlated Targets: Orbits Fits, TLEs, Magnitudes and Characteristic Lengths

| SSN of CT combo | Nights Obs TLE | MM (days) | Ecc | Inc (°) | RAAN (°) | DELVEC (arcsec) | Mag (V) | Lc (cm) |
|--------------------|-------------------|----------------------|------------------|----------------|------------------|--------------------|------------|------------|
| 2867 " | 1 TLE | 1.102396 1.091656 | 0.0 0.0051 | 10.26 10.26 | 331.82 331.89 | --- | 11.50 | 555 |
| 3431 " | 5 TLE | 1.003313 1.003320 | 0.0356 0.0010 | 10.74 10.92 | 335.03 335.00 | 4.19 | 13.72 | 200 |
| 3432 " | 5 TLE | 1.015158 1.015140 | 0.0760 0.0095 | 10.71 10.38 | 333.51 333.53 | 0.98 | 12.30 | 385 |
| 4250 " | 5 TLE | 1.002662 1.002692 | 0.1548 0.0023 | 11.54 12.14 | 334.99 335.19 | 6.04 | 16.21 | 63 |
| 4353 " | 5 TLE | 1.002673 1.002700 | 0.0705 0.0001 | 12.00 12.29 | 338.94 338.93 | 4.73 | 15.86 | 74 |
| 4902 " | 5 TLE | 1.002689 1.002719 | 0.0423 0.0001 | 13.10 13.29 | 340.01 339.99 | 3.43 | 15.22 | 100 |

The linkages between observations on subsequent nights was done by comparing the ACO parameters and combining nightly observations with similar orbit parameters and observed V magnitudes. The value of DELVEC was the determinant for viable eccentric orbit fits. Bad fits were easily recognized with DELVEC values from 100 to >1000 arcseconds. Due to the similarity of the orbits some targets linked up in more than one combination with DELVEC values of 20-100 arcseconds, but in all cases there was a linkage for a particular observation that had a DELVEC of less than 10 arcseconds. These potential linkages are summarized in Table 3. The orbital parameters presented in Table 3 correspond to the minimum DELVEC solution from a series of computer runs for each combination. In general the values of the mean motion (MM), INC and RAAN were stable, but the value of the eccentricity varied significantly between runs.

Table 3. Linked Potential Titan Fragments: Orbit Fits, Magnitudes and Characteristic Lengths

| UCT combo | Nights obs | MM (days) | Ecc | Inc (°) | RAAN (°) | DELVEC (arcsec) | Mag (V) | Lc (cm) |
|--------------|---------------|--------------|--------|------------|-------------|--------------------|------------|------------|
| A | 4 | 1.009593 | 0.0277 | 10.53 | 334.32 | 6.15 | 17.64 | 33 |
| B | 4 | 1.022732 | 0.0009 | 10.42 | 333.49 | 4.85 | 16.99 | 44 |
| C | 3 | 0.995522 | 0.0144 | 13.55 | 338.02 | 1.74 | 13.81 | 192 |
| D | 3 | 1.019077 | 0.0224 | 9.37 | 324.39 | 2.00 | 12.88 | 293 |
| E | 3 | 1.011477 | 0.0360 | 10.42 | 333.99 | 4.57 | 16.74 | 57 |
| F | 3 | 1.051054 | 0.0163 | 10.21 | 330.10 | 8.47 | 18.67 | 20 |
| G | 2 | 1.059044 | 0.0416 | 10.55 | 329.69 | 4.79 | 17.91 | 29 |
| H | 2 | 1.054224 | 0.0242 | 9.95 | 327.90 | 0.70 | 17.12 | 42 |
| I | 2 | 0.995524 | 0.0668 | 13.21 | 338.00 | 2.06 | 12.56 | 341 |

These linked combinations of UCTs are plotted in Figs. 9 and 10 along with the Titan fragments predicted by LEGEND modeling for February 2007. The UCTs fall well within the predicted regions for Titan debris including the two objects with mean motions less than 1 day. The eccentricity values are likely to be systematically high based on the comparison of the observed and TLE eccentricities for CTs. Such a good fit lends a high level of credence to the conclusion that we are observing Titan debris. The observed characteristic lengths (20-341cm) are representative of the sizes predicted by the LEGEND modeling.

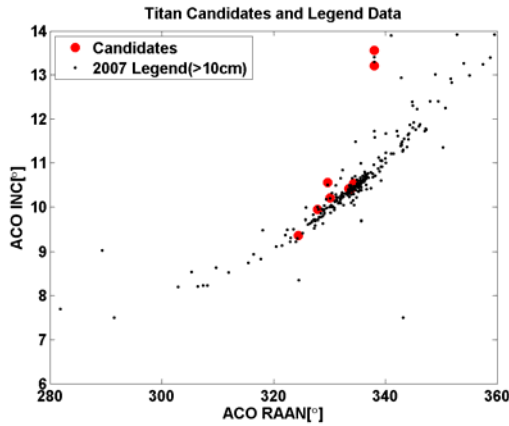


Fig. 9. Inclination- RAAN of Titan debris candidates and the LEGEND fragments for February 2007.

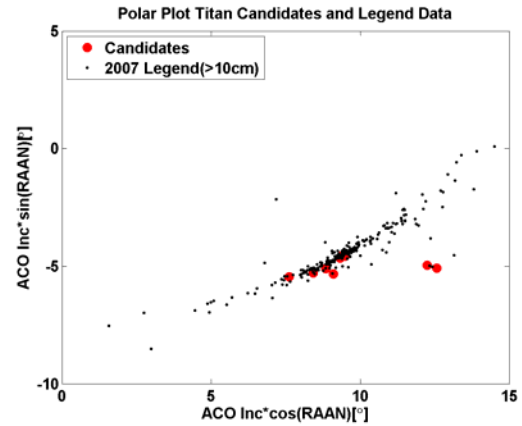


Fig.10. Polar plot Titan debris candidates and the LEGEND fragments for February 2007.

7. SUMMARY

Our observational program carried out with MODEST during February 2007 has detected 62 objects with a specialized stacking algorithm. Combinations of these detections over a period of six nights were linked together using a six parameter orbit fitting program to produce orbits for 15 unique targets. Six of these targets were correlated to cataloged targets with similar TLEs. Nine of the linked targets which were observed on 2 or more nights could not be correlated with cataloged targets. These candidates for Titan fragments have the same mean motion, inclination and RAAN values as the modeled Titan breakup fragments which have been propagated to the February 2007 epoch.

Future work on these particular Titan fragments is not feasible because accurate orbits could not been determined from these limited observations. However, we could apply our 2 telescope survey and follow-up program (presented at this conference) [13] to determine colors and more accurate orbits in an attempt to characterize the physical nature of the debris from the breakup of the Titan-3C transtage.

7. REFERENCES

1. Barker E., et al., Results from the NASA/Michigan GEO Debris Survey, *Proceedings of AMOS 2006 Technical Conference Proceedings*, Maui, Hawaii, pp. 594-604, 2006.
2. Seitzer, P., et al., A Survey for Space Debris in Geosynchronous Orbit., *Proceedings of AMOS 2001 Technical Conference*, Maui, Hawaii, 2001.
3. Seitzer, P., et al., Results from the NASA/Michigan GEO Debris Survey, *Proceedings of AMOS 2004 Technical Conference Proceedings*, Maui, Hawaii, pp. 213-214, 2005.
4. *Numerical Recipes in Fortran 77 The Art of Scientific Computing*, 2nd Edition, Vol. 1, Cambridge University Press, p. 403, 1992.
5. Schildknecht, T., et al., Optical Observations of Space Debris in High-Altitude Orbits, *Proceedings of the Fourth European Conference on Space Debris*, ESA SP-587, Darmstadt, Germany, pp. 113 - 118, 2005.
6. Liou, J.-C., et al., LEGEND – A three-dimensional LEO-to-GEO debris evolutionary model, *Adv. Space Research*, Vol. 34, No. 5, pp. 981-986, 2004.
7. Liou, J.-C., Collision Activities in the Future Orbital Debris Environment. *Adv. Space Research*, Vol. 38, No. 9, pp. 2102-2106, 2006.
8. Johnson, N.L., et al., NASA's new breakup model of EVOLVE 4.0, *Adv. Space Research*, Vol. 28, No. 9, pp. 1377-1384, 2001.
9. <http://iraf.noao.edu/>
10. Yanagisawa, T., et al., Automatic Detection Algorithm for Small Moving Objects, *Publications Astron. Soc. Japan*, 57, pp.399-408, 2005.
11. Barker, E., et al. Analysis of Working Assumptions in the Determination of Populations and Size Distributions of Orbital Debris from Optical Measurements, *Proceedings of the 2004 AMOS Technical Conference*, Wailea, Maui, HI, pp. 225-235, 2004.
12. Mulrooney, M. and M. J. Matney, Derivation and Application of a Global Albedo yielding an Optical Brightness To Physical Size Transformation Free of Systematic Errors, *Proceedings of the 2007 AMOS Technical Conference*, Wailea, Maui, HI, this conference , September 12-15, 2007.
13. Seitzer, P., et al., Optical Studies of Space Debris at GEO - Survey and Follow-up with Two Telescopes, *Proceedings of the 2007 AMOS Technical Conference*, Wailea, Maui, HI, this conference, September 12-15, 2007.